Solar-Terrestrial Physics. 2026, vol. 12, iss. 1, pp. 22–28. DOI: 10.12737/stp-121202604. © 2026 K.A. Sidorenko, A.A. Vasenina. Published by INFRA-M Academic Publishing House

DOI: 10.12737/stp-121202604
EDN: XGYRMH

Received July 15, 2025
Accepted October 24, 2025

STUDYING THE INFLUENCE OF GEOMAGNETIC STORMS ON PARAMETERS OF THE IONOSPHERIC F2 LAYER DURING SOLAR ACTIVITY CYCLE 24

K.A. Sidorenko
Institute of Radiophysics and Physical Electronics Omsk Scientific Center SB RAS, Omsk, Russia, sidorenko.klim@yandex.ru

A.A. Vasenina
Institute of Radiophysics and Physical Electronics Omsk Scientific Center SB RAS, Omsk, Russia, vas.al.an@rambler.ru

Abstract. This paper presents the results of a study on the behavior of parameters of the ionospheric F2 layer, such as the critical frequency (f_oF2) and the peak height of the layer (h_mF2), under geomagnetic storms of varying intensities. The study is based on vertical sounding measurements from the DIDBase database and the *Dst* index calculated by the World Data Center for Geomagnetism. We examine a methodology for identifying the presence of a geomagnetic storm using *Dst*-index time series. The main patterns of f_oF2 and h_mF2 variations for different geographic latitudes, seasons, and storm intensities are identified and analyzed. The obtained results can be useful for forecasting and modeling ionospheric conditions, which is of great importance for various applications, including satellite communications, global positioning systems, and shortwave radio communications.

Keywords: F2-layer critical frequency, F2-layer peak height, geomagnetic activity, *Dst* index.

INTRODUCTION

Geomagnetic storms, which arise due to the complex relationship of the solar wind with the geomagnetic field, are among the most dynamic and energy-intensive processes in the solar-terrestrial system. When a solar wind charged particle flux passes through the magnetosphere, it causes significant changes in the electron structure of the ionosphere, especially in the F2 layer, which leads to fluctuations in its critical frequency f_oF2 and height of maximum electron density h_mF2 [Forbes et al., 2000; Araujo-Pradere et al., 2005].

Variations in the electron density, f_oF2, and h_mF2 directly affect the conditions for radio wave propagation through the ionosphere. While geomagnetic storms are in progress, the range of acceptable frequencies for HF radio signals both expands and critically narrows. A shift in h_mF2 indicates a change in the reflecting boundary, which can cause unpredictable changes in signal propagation paths and hence negatively affect the reliability of radio communications [Brunelli, Namgaladze, 1988; Danilov, 2001; Ratovsky et al., 2018; Danilov, Konstantinova, 2020].

A number of studies on the influence of geomagnetic storms on the ionosphere analyze variations in the parameters over certain territories [Berényi et al., 2018, 2023; Arowolo et al., 2021] during selected local time periods [Solomon et al., 2013; Kumar, Kumar, 2014] and at certain storm intensities [Chen et al., 2022]. When organizing communication systems, especially in an HF band, it is necessary to take into account global variations in f_oF2 and h_mF2. To comprehensively assess the effect of geomagnetic storms on radio systems, the behavior of the F2-layer parameters was analyzed during solar activity (SA) cycle 24 from 2009 to 2019. The study of variations in f_oF2 along with the dynamics of h_mF2 allows us not only to trace the response of the ionosphere to external cosmic disturbances, but also to identify correlation relationships between storm intensity and changes in the ionospheric structure. The data plays a key role both in optimizing the operating modes of radio communications and in modeling processes associated with SA. In addition, the results of this study will be used to improve the accuracy of neural network models of predicting ionospheric parameters, which have been developed in [Sidorenko et al., 2023].

1. GEOMAGNETIC STORM IDENTIFICATION ALGORITHM

The *Dst* index, which reflects changes in the geomagnetic field caused by ring currents in the magnetosphere during storms, has been chosen as a quantitative measure of geomagnetic storm intensity. The *Dst* data was taken from the archive of the World Data Center for Geomagnetism in Kyoto [https://wdc.kugi.kyoto-u.ac.jp/dstdir/index.html].

Determination of the presence of a geomagnetic storm is based on the analysis of *Dst* time series. The proposed approach employed a threshold value of Dst=–30 nT: all consecutive measurements corresponding to the condition Dst<–30 nT were considered to be potential candidates for classification as a geomagnetic storm [Danilov, 2013]. Besides, the criterion of minimum duration of continuous threshold crossing equal to 5 hrs was applied which made it possible to exclude random noises and short-term oscillations that do not have considerable physical significance for storm formation.

Since a magnetic storm can occur in the form of several closely spaced phase intervals, the next stage of the method involves combining such intervals. If there were less than 10 hrs between the intervals, they were aggregated in a single event. This approach reflects the physical reality, where a single storm event can have a complex structure with transitional stages between its main phases. When choosing the time intervals, we relied on the mean ones of the storm main phase, which is ~5–10 hrs [Akasofu, Chapman, 1975].

To characterize the magnetic storm in detail, the intervals of identified events were expanded due to inclusion of preliminary and subsequent quiet periods (Figure 1). This comprehensive approach provides not only high-quality identification of geomagnetic storms, but also a detailed understanding of their effect on ionospheric parameters.

Figure 1 illustrates variations in *Dst* (*a*) and f_oF2 (*b*) from 00:00 UT on April 11 to 23:00 UT on April 18, 2012 according to data from the PA836 ionosonde (34.8° N, 120.5° W). The period of the magnetic storm, which lasted from 10:00 UT on April 14 to 22:00 UT on April 15, 2012, is highlighted in orange.

According to the accepted international classification, minor storms are characterized by *Dst*>–50 nT; moderate, –50÷ –100 nT; strong, –100÷–200 nT; and extreme, *Dst*<–200 nT [Danilov, 2013]. Figure 2 illustrates the distribution of geomagnetic storms in solar cycle 24 from January 2009 to December 2019.

Taking into account the accepted classification, from processed data on 2009–2019 we have identified 211 geomagnetic storms: 71 minor, 118 moderate, 20 strong, and 2 extreme.

The Digital Ionogram Database (DIDBase) [https://giro.uml.edu/didbase/] was used to obtain measurement data on f_oF2 and h_mF2 during geomagnetic storms and quiet days. The statistical analysis was based on data from only those ionosondes that worked steadily during the entire period of the geomagnetic storm in question. The research employed measurements with 43 ionosondes. Below are their names, URSI codes (in parentheses), and geographical coordinates.

There are 7 ionosondes at high latitudes: Nord Greenland (NDA81) — 81.4° N, 17.5° W; Thule/Qaanaaq (THJ77) — 77.5° N, 69.2° W; Tromsø (TR169) — 69.6° N, 19.2° E; Norilsk (NO369) — 69.2° N, 88.0° E; Sondrestrom (SMJ67) — 67.0° N, 50.9° W; College AK (CO764) — 64.9° N, 148.0° W; Yakutsk (YA462) — 62.0° N, 129.6° E.

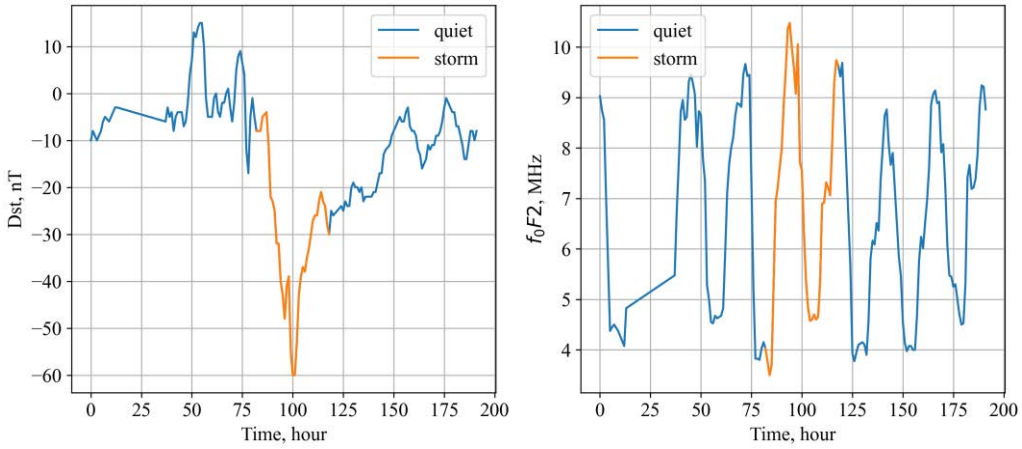

Figure 1. The *Dst* index (*a*) and f_oF2 (*b*) during a geomagnetic storm

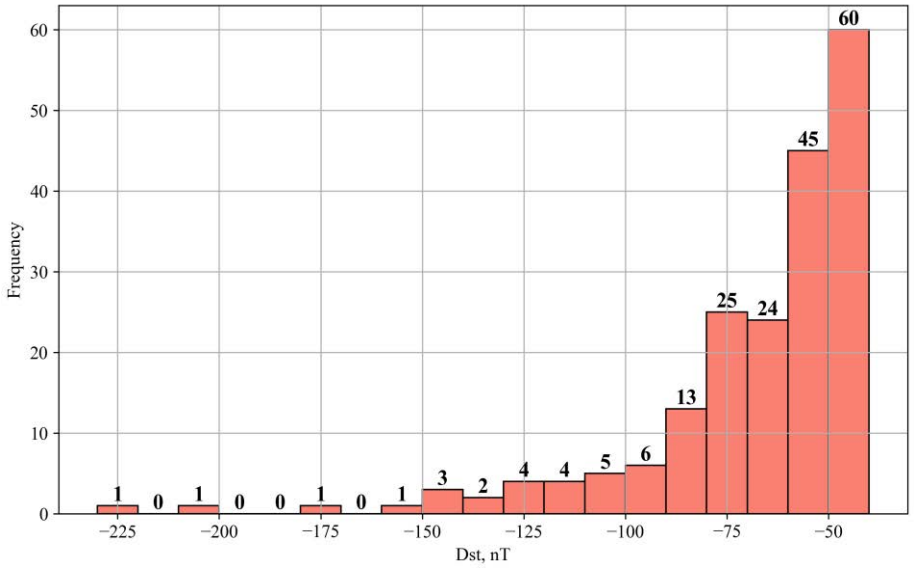

Figure 2. Distribution of geomagnetic storms

At midlatitudes are 24 ionosondes: King Salmon (KS759) — 58.4° N, 156.4° W; Moscow (MO155) — 55.5° N, 37.3° E; Juliusruh (JR055) — 54.6° N, 13.4° E; Goose Bay (GSJ53) — 53.3° N, 60.3° W; Irkutsk (IR352) — 52.4° N, 104.3° E; Fairford (FF051) — 51.7° N, 1.5° W; Chilton (RL052) — 51.5° N, 0.6° W; Dourbes (DB049) — 50.1° N, 4.6° E; Pruhonice (PQ052) — 50.0° N, 14.6° E; Millstone Hill (MHJ45) — 42.6° N, 71.5° W; Rome (RO041) — 41.9° N, 12.5° E; Roquetes (EB040) — 40.8° N, 0.5° E; San Vito (VT139) — 40.6° N, 17.8° E; Boulder (BC840) — 40.0° N, 105.3° W; Athens (AT138) — 38.0° N, 23.5° E; Wallops Is (WP937) — 37.9° N, 75.5° W; El Arenosillo (EA036) — 37.1° N, 6.7° W; Nicosia (NI135) — 35.0° N, 33.2° E; Port Arguello (PA836) — 34.8° N, 120.5° W; Eglin AFB (EG931) — 30.5° N, 86.5° W; Austin (AU930) — 30.4° N, 97.7° W; Port Stanley (PSJ5J)-51.6° S, 57.9° W; Grahamstown (GR13L) — 33.3° S, 26.5° E; Hermanus (HE13N) — 34.4° S, 19.2° E.

At low latitudes are 12 ionosondes: Ramey (PRJ18) — 18.5° N, 67.1° W; Kwajalein (KJ609) — 9.0° N, 167.2° E; Boa Vista (BVJ03) — 2.8° N, 60.7° W; Sao-luis (SAA0K) — 2.6° S, 44.2° W; Ascension Island (AS00Q) — 8.0° S, 14.4° W; Fortaleza (FZA0M) — 3.9° S, 38.4° W; Jicamarca (JI91J) — 12.0° S, 76.8° W; Campo Grande (CGK21) — 20.5° S, 55.0° W; Learmonth (LM42B) — 21.8° S, 114.1° E; Madimbo (MU12K) — 22.4° S, 30.9° E; Cachoeira Paulista (CAJ2M) — 22.7° S, 45.0° W; Louisvale (LV12P) — 28.5° S, 21.2° E.

2. ANALYSIS OF THE RESEARCH

To assess the response of f_oF2 and h_mF2 to geomagnetic storms, we calculated percentage changes in the daily peak of f_oF2 and h_mF2:

$$\Delta f_o F2 = \left(f_o F2_{storm} - f_o F2_{baseline}\right) / f_o F2_{baseline}, \quad (1)$$

$$\Delta h_m F2 = \left(h_m F2_{storm} - h_m F2_{baseline}\right) / h_m F2_{baseline}, \quad (2)$$

where $f_o F2_{storm}$, $h_m F2_{storm}$ are maximum daily values during the geomagnetic storm; $f_o F2_{baseline}$, $h_m F2_{baseline}$ are average maximum daily values during the quiet period lasting for three days before and three days after the geomagnetic storm.

The results are presented in Figures 3–6. We used a boxplot to visualize the data distribution. The main elements of this plot include the box itself, which covers the interquartile range — the difference between the first and third quartiles (spread of central 50 % of the data); whiskers representing lines coming from the box and demonstrating the data range of 5 percentiles (lower whisker) and 95 percentiles (upper whisker); outliers are data points located beyond the whiskers, indicating a spread of extreme 5 % of the data. A line indicating the median is displayed inside the box. When grouping by latitude, the following classification was made: high latitudes $|\varphi|>60°$, middle latitudes $30°<|\varphi|<60°$, and low latitudes $|\varphi|<30°$, where φ is the geographic latitude.

Figure 3 exhibits averages of the relative deviation of the critical frequency $<\Delta f_o F2>$ depending on season during geomagnetic storms for different latitudes. Midlatitudes are seen to feature an increase in the critical frequency during this period: there are positive changes in the median value of the average relative deviation of the critical frequency $M<\Delta f_o F2>$.

The greatest effect occurs in winter when $M<\Delta f_o F2>$ runs to +6.0 %, whereas in spring it is +3.6 %. A similar trend is observed for low latitudes: the greatest effect is in winter — +6.6 %, in spring — +4.0 %. For high latitudes, an increase in f_oF2 was recorded only in winter (to +2.4 %), whereas in spring, summer, and autumn there is a tendency for f_oF2 to decrease from –7.4 to –10.8 %.

Figure 4 plots $<\Delta f_o F2>$ depending on the geomagnetic storm intensity.

At high latitudes during minor geomagnetic storms, there is a slight positive effect $M<\Delta f_o F2>$ amounting to +1.2 %. During moderate geomagnetic storms, $M<\Delta f_o F2>$ decreases to –9.2 % nonetheless. During strong storms, the effect increases, running to –21.4 %;

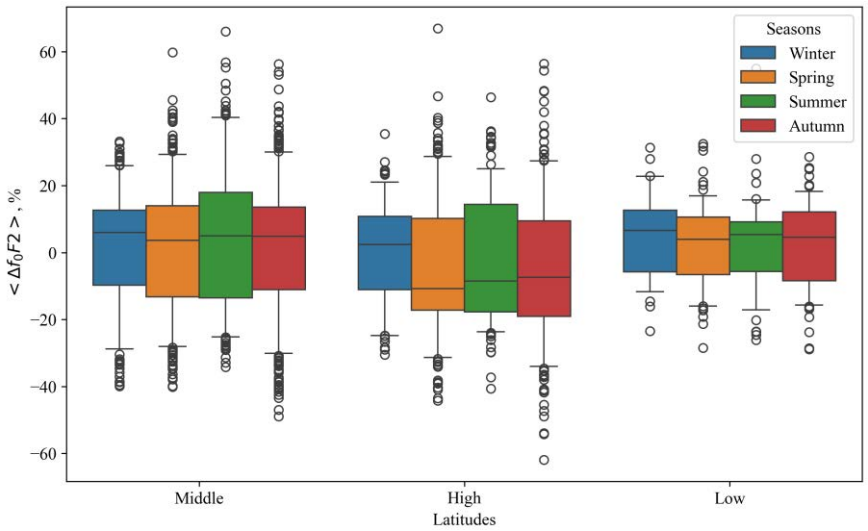

Figure 3. Variations $<\Delta f_o F2>$ depending on season during geomagnetic storms for different latitudes

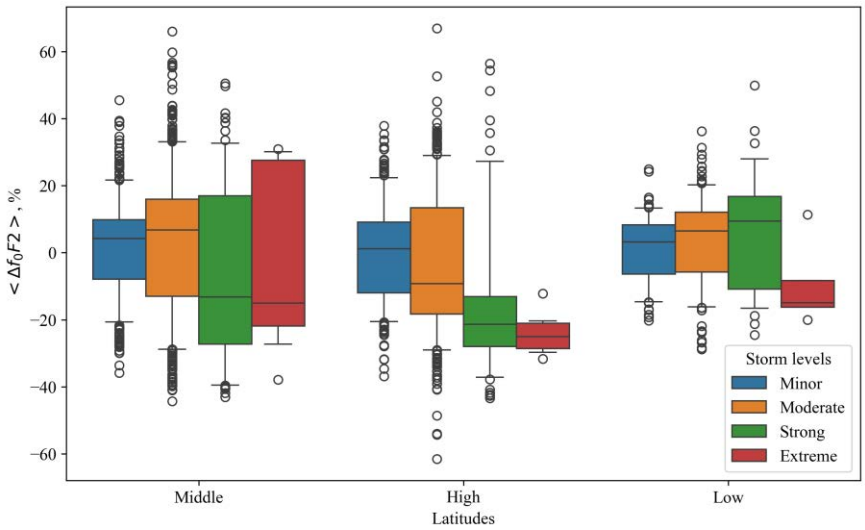

Figure 4. Variations <Δf_oF2> depending on the geomagnetic storm intensity for different latitudes

and extreme disturbances lead to an even more significant decrease to –25.0 %. This phenomenon is physically explained by a change in the neutral atmosphere composition, in particular a decrease in the ratio of atomic oxygen concentration to the nitrogen one [Danilov, 2013; Ratovsky et al., 2018; Chernigovskaya et al., 2024].

At midlatitudes during minor and moderate geomagnetic storms, a positive effect M<Δf_oF2> is observed which amounts to +4.2 and +6.8 % respectively. The increase in f_oF2 is due to the appearance of additional wind, which improves ionization of the upper ionosphere [Danilov, 2013; Ratovsky et al., 2018; Danilov, Konstantinova, 2020]. The effect, however, becomes negative, running to –13.2 and –15.0 %, during strong and extreme storms. Note that the statistical reliability of extreme storm data is limited to a small sample.

At low latitudes, geomagnetic storms (from minor to strong) bring about positive changes in M<Δf_oF2>: from +3.2 % for minor to +9.5 % for strong. The positive effect is driven by an increase in the equatorial fountain effect and disturbing electric fields that cause the F2 layer to rise to a height with a lower recombination rate [Danilov, Konstantinova, 2020; Chernigovskaya et al., 2024]. During extreme storms, this effect is, however, inverted: M<Δf_oF2> reaches –15.0 %, which may suggest that the normal dynamics of the ionosphere is affected. In particular, during the strongest geomagnetic storm of solar cycle 24 in March 2015, which lasted throughout the recovery phase, a change from a positive effect to a negative one was detected during the magnetic storm main phase [Chernigovskaya et al., 2024]. Due to the small number of extreme storms, it is impossible to collect statistical data in view of specifics for different seasons.

For a more convenient analysis of the ionosphere behavior, Table 1 lists M<Δf_oF2>, σ<Δf_oF2>, as well as max<Δf_oF2> and min<Δf_oF2>.

A significant standard deviation σ<Δf_oF2> from ~9 to ~26 % indicates that individual geomagnetic events vary. This suggests that individual events may differ significantly in intensity and duration of impact on f_oF2, which calls for additional analysis of storm intensity.

Next, we turn to the analysis of the relationship between averages of <Δh_mF2>. Figure 5 shows <Δh_mF2> grouped by latitude and season.

All latitudes are seen to be marked by an increase in h_mF2 during geomagnetic storms: positive changes in M<Δh_mF2> are recorded. For middle and high latitudes, M<Δh_mF2> varies from +6.6 to +9.5 %. At the same time, for low latitudes such a high level is recorded only in summer; in winter, spring, and autumn, M<Δh_mF2> varies from +1.3 to +3.7 %.

Table 1

Statistical data on <Δf_oF2>

<Δf_oF2>, %	Middle latitudes				High latitudes				Low latitudes			
	M	σ	max	min	M	σ	max	min	M	σ	max	min
Season												
winter	6.0	16.4	33.2	–39.9	2.4	14.8	35.4	–30.5	6.6	11.5	31.4	–23.4
spring	3.6	18.0	59.8	–40.1	–10.8	19.1	66.9	–44.3	4.0	11.5	32.5	–28.4
summer	5.0	20.5	66.0	–34.2	–8.6	18.4	46.4	–40.6	5.4	13.0	55.0	–26.1
autumn	4.9	18.3	56.3	–48.9	–7.4	19.8	56.4	–61.9	4.6	12.2	28.6	–28.9
Magnetic storm intensity												
minor	4.2	13.1	45.5	–35.8	1.2	13.7	37.9	–36.9	3.2	9.3	24.9	–20.2
moderate	6.8	19.6	66.0	–44.3	–9.2	19.9	66.9	–61.5	6.5	12.0	36.2	–28.9
strong	–13.2	25.1	50.5	–43.0	–21.4	21.2	56.4	–43.4	9.4	17.2	50.0	–24.5
extreme	–15.0	26.2	30.9	–37.9	–25.0	6.0	–12.2	–31.7	–15.0	14.2	11.3	–20.1

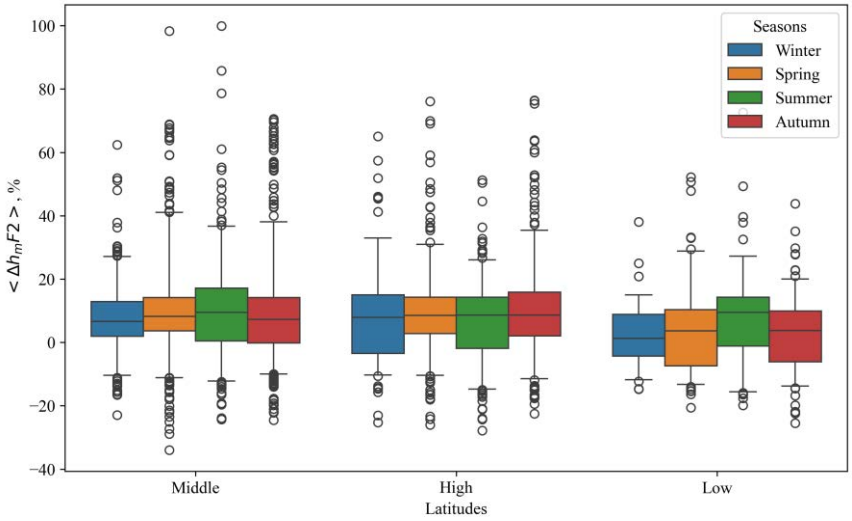

Figure 5. Variations <Δh_mF2> depending on season during geomagnetic storms for different latitudes

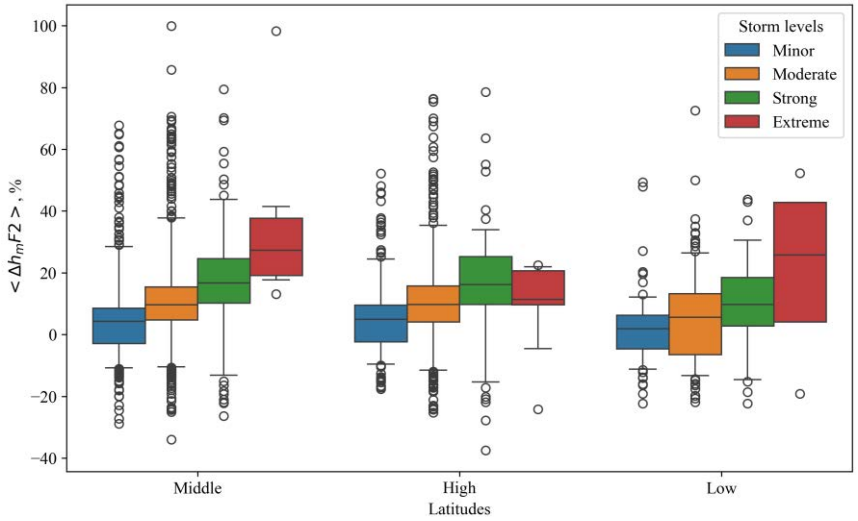

Figure 6. Variations <Δh_mF2> versus the geomagnetic storm intensity for different latitudes

The data (Figure 6) shows that as a magnetic disturbance increases, h_mF2 rises markedly, especially during strong storms. At middle and low latitudes, extreme storms cause the layer to rise significantly; at high latitudes, extreme storms reveal a slight decrease compared to strong storms.

Initial values of h_mF2 are set by the seasonal background, which depends on the thermosphere temperature and composition: in summer, it is higher; in winter, lower. The effects produced by geomagnetic storms (direct effects of fields and thermosphere dynamics) are superimposed on the seasonal level. They create an additional rise [Danilov, 2013; Ratovsky et al., 2018; Danilov, Konstantinova, 2020]. These effects are most pronounced in midlatitudes and at the equator.

The combined effect of seasonality and geomagnetic disturbances determines the observed variations in h_mF2: the combination of the summer period and a strong storm leads to a general rise in M<Δh_mF2> to 20–30 %, whereas in winter, even during strong storms, the rise is only 5–10 %.

For convenience, Table 2 presents M<Δh_mF2>, σ<Δh_m F2>, as well as max<Δh_mF2> and min<Δh_mF2>, h_mF2 is also characterized by significant σ<Δh_mF2> (from ~10 to ~31 %), which indicates the variability of individual geomagnetic events.

There is a moderate negative correlation between f_oF2 and h_mF2 in general, especially during daytime hours and at high SA: when the electron density rises, f_oF2 increases, and h_mF2, as a rule, decreases because ionization is more intense at lower altitudes. On the contrary, when ionization decreases (at night or at low SA), h_mF2 goes up, and f_oF2 goes down. At midlatitudes, the correlation between f_oF2 and h_mF2 can range from –0.3 to –0.7, depending on time and SA conditions. Let us estimate the relationship between the F2-layer parameters during magnetic storms (see Figure 7).

During geomagnetic storms, the relationship is seen to weaken significantly; during strong storms, the correlation coefficient is <0.1. Analysis of the relationships (Figures 3–6) reveals that as magnetic storms intensify (especially at high latitudes) there is a tendency for f_oF2 to decrease and for h_mF2 to increase at a time. This can be interpreted as a vertical motion and redistribution of plasma — the effect, where a rise of the layer leads to a decrease in density at the peak point. In the middle and equatorial zones during minor and moderate storms, f_oF2 can exhibit positive values (an increase in ionospheric density).

Table 2

Statistical data on $<\Delta h_m F2>$

$<\Delta h_m F2>$, %	Middle latitudes				High latitudes				Low latitudes			
	M	σ	max	min	*M*	σ	max	min	*M*	σ	max	min
Season												
winter	6.6	12.1	62.4	–22.9	7.8	15.3	65.0	–25.2	1.3	10.1	38.0	–14.8
spring	8.2	15.6	98.3	–34.0	8.5	13.9	76.1	–26.0	3.6	14.1	52.2	–20.6
summer	9.5	16.5	99.9	–24.3	8.6	13.0	51.2	–27.8	9.5	14.6	72.6	–19.9
autumn	7.2	15.4	70.6	–24.5	8.6	15.8	76.4	–22.5	3.7	11.8	43.8	–25.5
Magnetic storm intensity												
minor	4.3	12.9	67.7	–28.9	5.0	10.9	52.1	–17.6	1.8	9.9	49.3	–22.4
moderate	9.6	14.8	99.9	–34.0	9.8	15.2	76.4	–25.2	5.6	13.8	72.6	–21.9
strong	16.7	17.1	79.4	–26.4	16.2	17.6	78.6	–37.5	9.7	15.3	43.8	–22.3
extreme	27.3	21.0	98.3	13.1	11.4	15.4	22.5	–24.2	25.7	31.7	52.2	–19.1

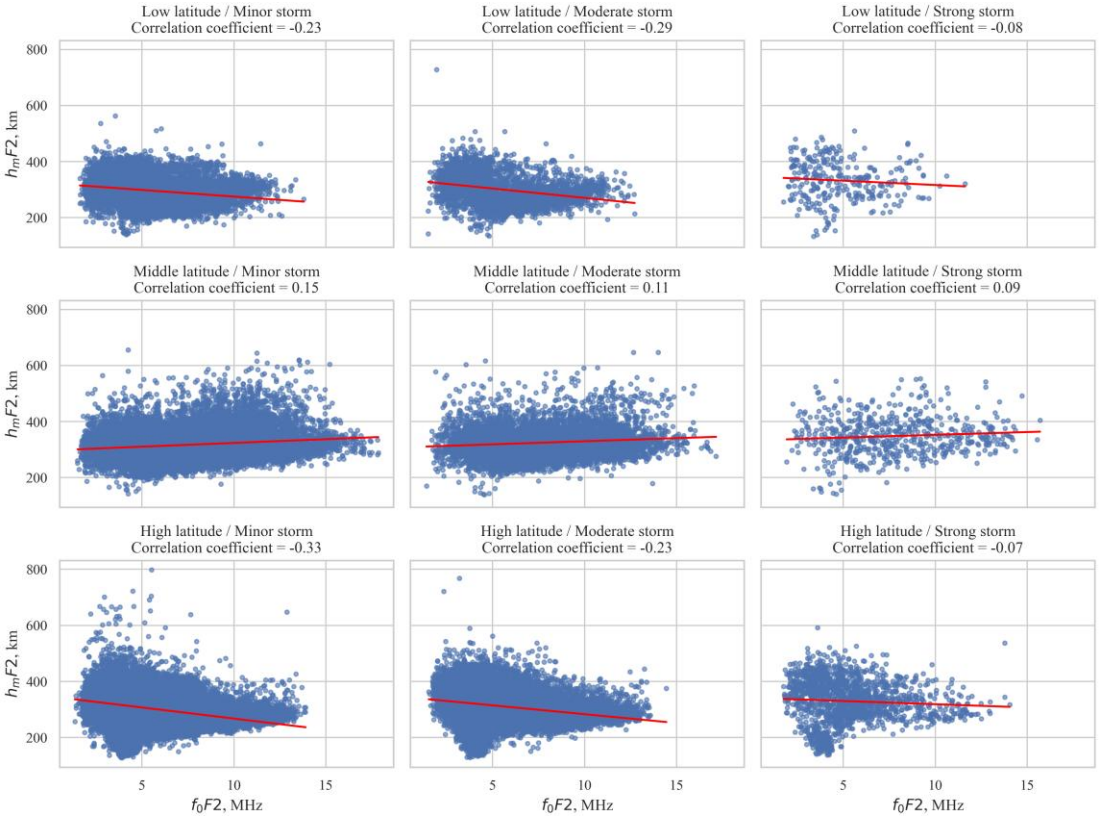

Figure 7. Correlation between f_oF2 and h_mF2 for different latitudes and geomagnetic storms

CONCLUSION

The experimental results have shown that geomagnetic storms have a different effect on the F2 layer depending on the geographical location, season, and storm intensity.

1. At high latitudes, f_oF2 decreases, especially in spring ($M<\Delta f_oF2>$=–10.8 %), summer ($M<\Delta f_oF2>$=–8.6 %), and autumn ($M<\Delta f_oF2>$=–7.4 %). In terms of storm categories, a considerable decrease in f_oF2 is noticeable during strong and extreme storms (–21.4 and –25.0 % respectively).

2. Midlatitudes demonstrate a positive effect $M<\Delta f_oF2>$ (to +6.8 %) for minor and moderate storms, as well as for all seasons (from +3.6 to +6.0 %), but during strong storms the effect changes to a negative one (–13.2 %).

3. Positive changes $M<\Delta f_oF2>$ are also observed in the equatorial zone, with the effect increasing in winter (+6.6 %). Extreme disturbances can, nonetheless, disrupt the standard dynamics and lead to a decrease in $M<\Delta f_o$ F2> to –15.0 %.

4. Significant deviations (in some cases, more than 60 %) indicate the variability of individual geomagnetic disturbances. This suggests that individual events can differ significantly in intensity and duration of the effect on f_oF2.

5. As the geomagnetic storm intensity grows, the F2-layer maximum rises in all categories. These changes are especially pronounced in the middle and equatorial regions, where extreme storms can increase $<\Delta h_m F2>$ to very high values (for example, +27.3 % at midlatitudes).

6. During minor storms, the F2-layer height is much lower, which emphasizes the dynamic behavior of the ionospheric layer when exposed to external disturbances.

7. During strong magnetic storms, the relationship between f_oF2 and h_mF2 decreases significantly (the correlation coefficient is less than 0.1).

8. There is a relationship between a decrease in f_oF2 and an increase in h_mF2 during magnetic storms at high latitudes. This can be interpreted as the result of a vertical redistribution of ions when enhanced electric fields and atmospheric waves cause the peak layer to shift to a higher altitude, which leads to a decrease in the local concentration.

Thus, when predicting the influence of the ionosphere on radio wave propagation during geomagnetic storms, it is necessary to take into account the intensity of the geomagnetic storm on its own, the geographical latitude of the path, and season. The results will be used for follow-up studies of ionospheric variability and the possibility of improving its forecast precision.

The work was performed on the Government Assignment of the Omsk Scientific Center SB RAS (Project State Registration Number 125013101211-4).

We would like to thank the organizations that acquire the ionospheric and magnetic data used in this work.

REFERENCES

Akasofu S.I., Chapman S. *Solnechno-zemnaya fizika* [Solar-Terrestrial Physics]. *Pt. 2.* Moscow, Mir Publ., 1975, 510 p. (In Russian).

Araujo-Pradere E.A., Fuller-Rowell T.J., Codrescu M.V., Bilitza D. Characteristics of the ionospheric variability as a function of season, latitude, local time, and geomagnetic activity. *Radio Sci*. 2005, vol. 40, RS5009, pp. 1–15. DOI: 10.1029/2004RS003179.

Arowolo O.A., Akala A.O., Oyeyemi E.O. Interplanetary origins of some intense geomagnetic storms during solar cycle 24 and the responses of African equatorial/low-latitude ionosphere to them. *J. Geophys. Res.: Space Phys.* 2021, vol. 126, iss. 2, pp. 1–20. DOI: 10.1029/2020JA027929.

Berényi K.A., Barta V., Kis A. Midlatitude ionospheric F2-layer response to eruptive solar events-caused geomagnetic disturbances over Hungary during the maximum of the solar cycle 24: A case study. *Adv. Space Res*. 2018, vol. 61, iss. 5, pp. 1230–1243. DOI: 10.1016/j.asr.2017.12.021

Berényi K.A., Heilig B., Urbář J., et al. Comprehensive analysis of the ionospheric response to the largest geomagnetic storms from solar cycle 24 over Europe. *Front. Astron. Space Sci.* 2023, vol. 10, pp. 1–22. DOI: 10.3389/fspas.2023.1092850.

Brunelli B.E., Namgaladze A.A. *Fizika ionosfery* [Physics of the Ionosphere]. Moscow, Nauka Publ., 1988, 528 p. (In Russian).

Chen Y., Liu L., Le H., et al. Responding trends of ionospheric F_2-layer to weaker geomagnetic activities. *J. Space Weather Space Climate.* 2022, vol. 12, no. 6, pp. 1–12. DOI: 10.1051/swsc/2022005.

Chernigovskaya M.A., Ratovsky K.G., Zherebtsov G.A., et al. Ionospheric response over the high and middle latitude regions of Eurasia according to ionosonde data during the severe magnetic storm in March 2015. *Sol.-Terr. Phys*. 2024, vol. 10, iss. 4, pp. 46–58. DOI: 10.12737/stp-104202406.

Danilov A.D. Ionospheric F-region response to geomagnetic disturbances. *Adv. Space Res*. 2001, vol. 52, iss. 5, pp. 441–449. DOI: 10.1016/S1364-6826(00)00175-9.

Danilov A.D. Reaction of F region to geomagnetic disturbances (Review). *Heliogeophys. Res.* 2013, iss. 5, pp. 1–33. (In Russian).

Danilov A.D., Konstantinova A.V. Long-term variations in the parameters of the middle and upper atmosphere and ionosphere. *Geomagnetism and Aeronomy.* 2020, vol. 60, iss. 4, pp. 397–420. DOI: 10.1134/S0016793220040040.

Forbes J.M., Palo S.E., Zhang X. Variability of the ionosphere. *J. Atmos. Solar-Terr. Phys.* 2000, vol. 62, iss. 8, pp. 685–693. DOI: 10.1016/S1364-6826(00)00029-8.

Kumar A., Kumar S. Space weather effects on the low latitude D-region ionosphere during solar minimum. *Earth, Planets and Space*. 2014, vol. 66, pp. 1–10. DOI: 10.1186/1880-5981-66-76.

Ratovsky K.G., Klimenko M.V., Klimenko V.V., et al. Aftereffects of geomagnetic storms: Statistical analysis and theoretical explanation. *Sol.-Terr. Phys*. 2018, vol. 4, iss. 4, pp. 26–32. DOI: 10.12737/stp44201804.

Sidorenko K.A., Vasenina A.A., Kondratyev A.N. Improving forecasting accuracy the F2-layer peak characteristics using artificial neural network. *Adv. Space Res*. 2023, vol. 71, iss. 8, pp. 3373–3381. DOI: 10.1016/j.asr.2022.12.006.

Solomon S., Qian L., Burns A. The anomalous ionosphere between solar cycles 23 and 24. *J. Geophys. Res.: Space Phys.* 2013, vol. 118, iss. 10, pp. 6524–6535. DOI: 10.1002/jgra.50561.

URL: https://giro.uml.edu/didbase/ (accessed September 15, 2025).

URL: https://wdc.kugi.kyoto-u.ac.jp/dstdir/index.html (accessed September 15, 2025).

Original Russian version: Veniaminov S.S., Kozlov S.I., Kuzmicheva M.Yu., published in Solnechno-zemnaya fizika. 2026, vol. 12, no. 1, pp. 25–32. DOI: 10.12737/szf-121202604.

How to cite this article

Sidorenko K.A., Vasenina A.A. Studying the influence of geomagnetic storms on parameters of the ionospheric F2 layer during solar activity cycle 24. *Sol.-Terr. Phys*. 2026, vol. 12, iss. 1, pp. 22–28. DOI: 10.12737/stp-121202604.